


Stability Testing of $\text{Pt}_x\text{Sn}_{1-x}/\text{C}$ Anodic Catalyst for Renewable Hydrogen Production Via Electrochemical Reforming of Ethanol

Ana B. Calcerrada¹ · Ana R. de la Osa¹ · Holly A. E. Dole² · Fernando Dorado¹ · Elena A. Baranova² · Antonio de Lucas-Consuegra¹ 

Published online: 16 October 2017
© Springer Science+Business Media, LLC 2017

Abstract The stability testing of three different synthesized $\text{Pt}_x\text{Sn}_{1-x}/\text{C}$ anodic catalysts has been demonstrated for the renewable generation of hydrogen via the electrochemical reforming of ethanol in a proton exchange membrane (PEM) electrolysis cell. Three Pt-Sn anodic catalysts with different nominal Pt:Sn ratios of 60:40, 70:30, and 80:20 atomic (at.) % were synthesized and characterized by the means of electrochemical tests and XRD. Among them, the Pt-Sn anodic catalyst with 70:30 at. ratio showed the highest electrochemical active surface area (ECSA) and highest electrochemical reforming activity, which allowed the production of pure H_2 with the lowest electrical energy requirement (below $23 \text{ kWh}\cdot\text{kg}_{\text{H}_2}^{-1}$). The stability of the system was also demonstrated through a long-term chronopotentiometry experiment of 48 h in duration. The potential for practical use and coupling this technology with renewable solar energy, a number of cyclic voltammetry tests (with a low scan rate of $0.19 \text{ mV}\cdot\text{s}^{-1}$) were also carried out. These experiments were performed by simulating the electrical power produced by a photovoltaic cell. This test showed good stability/reproducibility of the

MEA and, hence, a suitable integration between the two technologies for the sustainable energy storage in the form of hydrogen.

Keywords Pt-Sn catalyst · Ethanol electro-oxidation · Hydrogen production · Electrochemical reforming · Energy storage · Electrolysis

Introduction

In the last years, hydrogen has been considered as the most promising energetic vector to obtain clean and sustainable energy, especially considering some of the issues of fossil fuels as a resource [1]. Although, hydrogen can be obtained from a variety of processes and materials, it is mostly produced by steam reforming of methane. However, this process has several drawbacks and leads to production of a mixture of hydrogen and carbon based, CO and CO_2 . This results in the requirement for further separation and purification to be able to use the hydrogen. In response, the electrolysis process has gained more interest considering it generates pure hydrogen in one step [2]. However, as a practical application, it is limited by the high overpotential required for producing large amounts of hydrogen, which means higher energy consumption.

As an alternative, electrochemical reforming of alcohols has been shown to decrease this energy demand [2]. Electrical power is used to split organic molecules via electrooxidation in order to produce hydrogen. Due to the high energy contained in this type of fuel, the requirement of an external energy source is decreased. This allows for higher

Electronic supplementary material The online version of this article (<https://doi.org/10.1007/s12678-017-0428-0>) contains supplementary material, which is available to authorized users.

✉ Antonio de Lucas-Consuegra
Antonio.lconsuegra@uclm.es

¹ Chemical Engineering Department, Faculty of Chemical Sciences and Technology, University of Castilla-La Mancha, Avda. Camilo José Cela 12, 13071 Ciudad Real, Spain

² Department of Chemical and Biological Engineering, Center for Catalysis Research and Innovation (CCRI), University of Ottawa, 161 Louis-Pasteur St, Ottawa, ON K1N 6N5, Canada

current density values and lower anode potentials than that required for water electrolysis [2]. Recently, interesting results have been shown regarding the electrochemical reforming of water-alcohol mixtures, e.g., methanol [2–4], glycerol [5–7], ethanol [1, 8–11], bio-ethanol [12, 13], and ethylene glycol [14] at low temperature and at atmospheric pressure. In this process, electrolysis is carried out at potentials lower than 1.3 V, and the energy requirement is typically lower than that for water electrolysis. Pt-based bimetallic catalysts, e.g., PtRu and PtSn, are the most studied for this reaction [15–17]. The addition of the second metal (Ru, Sn, Mo) promotes the reaction through the bifunctional mechanism or/and electronic effect [15, 16]. Furthermore, the second metal decreases the surface poisoning and in some cases reduces the cost of the anodic catalyst for alcohol electrooxidation [15–17]. Among the Pt-bimetallic systems, PtSn catalysts have been found to show good performance for electrooxidation of ethanol [18, 19]. However, PtSn catalysts show controversial results depending on the Sn phase, Pt/Sn atomic ratio, particle size, dispersion, and synthesis procedure [18, 20]. Previous investigation by our group demonstrated the effects of these parameters with a Pt₇-Sn₃/C (70:30 at.% of Pt:Sn) anodic catalyst, synthesized using the polyol reduction method for the electroreforming of methanol, ethanol, and ethylene glycol [1].

The present work is a continuation of this study, aiming to evaluate the stability of Pt_xSn_{1-x}/C anodic catalyst for the hydrogen production via electrochemical reforming of ethanol, exploring the possibility of coupling of this technology with renewable energy sources, i.e., electrical power developed by a photovoltaic solar profile. Hence, we report a detailed investigation on the optimal Pt:Sn atomic ratio and the effect of alloying on the electrocatalytic performance. We correlate the optimal composition of three different Pt-Sn anodic catalysts and their physicochemical properties with the electrocatalytic activity for hydrogen production via electrochemical reforming of ethanol in a PEM electrolysis cell. Furthermore, we performed long-term experiments (chronoamperometry and cyclic voltammetry measurements) to demonstrate the stability and the durability of the system in view of possible practical applications.

Experimental Section

Catalyst Synthesis

The catalysts were synthesized using the polyol reduction method [19, 21, 22], using ethylene glycol (EG) as a stabilizing and reducing agent. EG also acted as a surfactant after precursor metal salt reduction, preventing any particle agglomeration after the formation of colloidal particles. The procedure was explained in detail elsewhere [1] and could be summarized as follows: First, platinum(IV) chloride (PtCl₄,

Alfa Aesar, 99.99% metals basis) and tin(II) chloride anhydrous (SnCl₂, Acros Organics, 98% anhydrous) were weighed according to the appropriated atomic ratio (i.e., Pt:Sn 60:40, 70:30, 80:20) and then dissolved in EG (99.8% anhydrous, Sigma-Aldrich) with a concentration of 0.2 M NaOH (EM Science, ACS grade). The solution was stirred for 1 h at room temperature and refluxed for 2 h at 190 °C (pH before, 11; pH after, 9). A corresponding mass (for the accurate 20 wt.% loading) of carbon black (Vulcan XC-72, Cabot corporation) was mixed with deionized water at room temperature. The Pt_xSn_{1-x} colloid was added to the carbon/water solution and stirred for 48 h at room temperature. Supported catalysts were extensively washed with deionized water (18 MΩ cm) and separated by centrifugation then dried in a freeze-dryer for 8 h.

Electrode and Membrane Electrode Assembly Preparation

The electrodes were formed of commercial carbon paper (Fuel Cell Earth) substrates and a catalyst layer deposited onto it as a catalyst ink. These inks were prepared by mixing appropriate amounts of the 20 wt.% Pt_xSn_{1-x}/C powder as the anode and Pt/C (20 wt.% Pt/C, Alfa Aesar) as the cathode electrocatalysts with a Nafion solution (5 wt.%, Sigma Aldrich) and isopropanol (99.9% for HPLC, Sigma-Aldrich). Inks were deposited on carbon paper to achieve a metal loading of 1.5 mg cm⁻² for the anode and 0.5 mg cm⁻² for the cathode. The geometric surface area was 0.53 cm² for the electrodes tested in the three-electrode electrochemical cell and 6.25 cm² for the case of the PEM electrolysis cell. In the latter case, the electrolyte consisted of a proton exchange membrane of 185 μm thickness (Hidrógena Desarrollos Energéticos). Prior to use, the polymeric membrane was pretreated by successive immersion at 100 °C for 2 h in H₂O₂ and H₂SO₄ solutions and deionized water. The membrane electrode assembly (MEA) was then prepared with hot pressing, under 1 metric ton at 120 °C for 3 min.

Catalyst Characterization

Anodic Catalyst Powder

Pt_xSn_{1-x}/C catalyst powders were characterized by X-ray diffraction to obtain the crystalline size using the Scherrer's formula and morphology of different anodic catalysts. The analysis was recorded on a Siemens Bruker D5000 XRD diffractometer, using Cu K_α radiation (λ = 1.54184 Å). Diffractograms were collected between 20° ≤ 2θ ≤ 100° with a step of 0.02° (scan time 2 s·step⁻¹) and compared with the JCPDS-ICDD references.

Anodic Catalyst Electrodes

In order to study the electrochemical behavior of different $\text{Pt}_x\text{Sn}_{1-x}/\text{C}$ electrodes, a voltammetric study was carried out in a three-electrode electrochemical glass cell (half cell), explained in detail elsewhere [10]. This test consisted of cyclic voltammetry (CV) measurements (-0.4 V to 1.2 V vs. Ag/AgCl) at $50 \text{ mV}\cdot\text{s}^{-1}$, in $0.5 \text{ M H}_2\text{SO}_4$ at 25°C with a platinum foil as a counter electrode and Ag/AgCl ($\text{KCl } 3 \text{ mol}\cdot\text{L}^{-1}$) (Metrohm) as a reference electrode. Before each test, the working solution was carefully purged with nitrogen for 1 h to remove O_2 from the electrolyte. This technique was used to determine the electrochemical surface area (ECSA) [23]. ECSA values were obtained by the H_2 desorption peak area, by Eq. 1 [24]:

$$\text{ECSA} = \frac{A_{\text{Pt}}}{\nu \cdot C} \cdot \frac{1}{L_e} \quad (1)$$

where A_{Pt} is the peak area ($\text{A}\cdot\text{V}\cdot\text{cm}^{-2}$), ν is the scan rate ($\text{V}\cdot\text{s}^{-1}$), C is the charge required to reduce the proton monolayer of the active platinum ($0.21 \text{ mC}\cdot\text{cm}^{-2}$), and L_e is the metal load in the catalyst layer ($1.5 \text{ mg}\cdot\text{cm}^{-2}$).

Electrochemical Reforming Measurements

PEM Electrolysis Cell

Experimental tests were carried out in a PEM electrolysis cell to demonstrate the activity and durability of $\text{Pt}_x\text{Sn}_{1-x}/\text{C}$ catalysts in the electroreforming of ethanol-water solutions. The experimental setup was described in detail elsewhere [8] (See Fig. S1 in the Supporting Information). The MEA was introduced between two Teflon gaskets to avoid short-circuiting and to ensure sealing between the anode and cathode chambers. Graphitic bipolar plates were placed on both sides of the MEA. These plates served as flow channels (parallel grooves, with a total surface area of 6.25 cm^2 , were drilled in them) and as current collectors. Finally, all the above items were placed between external Teflon plates covered with metallic end plates. Then, the system was uniformly tightened with nuts and bolts using an electronic torque wrench to ensure mechanical stability.

The electrochemical tests were carried out using a Vertex 5A.DC potentiostat-galvanostat, electrochemical analyzer (Ivium Technologies) controlled by software. The anodic compartment of the PEM cell was fed with $4 \text{ mol}\cdot\text{L}^{-1}$ ethanol/water solution at a constant flow rate of $10 \text{ mL}\cdot\text{min}^{-1}$ using a peristaltic pump (Pumpdrive 5001, Heidolph). Water was supplied to the cathode chamber using another peristaltic pump (Pumpdrive 5001, Heidolph) at a constant flow rate of $3 \text{ mL}\cdot\text{min}^{-1}$. Hydrogen production was quantified with a high-precision flowmeter (Flowmeter ADM 2000, Agilent

Technologies) and confirmed via Faraday's law. Both feeding solutions were preheated at a temperature close to that of the cell, which was always kept in a temperature range between 30 and 80°C .

Two variations of electrochemical experiments were performed: (a) linear sweep voltammetry measurements at a scan rate of $5 \text{ mV}\cdot\text{s}^{-1}$, up to a maximum applied potential of 1.4 V, and (b) mild-term galvanostatic experiment ($I = 0.1$ A) in six consecutive cycles (of 8 h of duration of each one) with open circuit potential conditions (of 5 min of duration) between them. Analysis of the gaseous cathodic products was carried out using a gas chromatograph (Bruker 450 GC) to confirm the hydrogen purity.

Three-Electrode Glass Cell

To assess the catalyst stability, an accelerated stress test (AST) was carried out in a three-electrode glass cell (half cell). Ag/AgCl ($\text{KCl } 3 \text{ mol}\cdot\text{L}^{-1}$) was used as reference electrode, the counter electrode was a platinum foil, and the working electrode was the Pt-Sn anodic catalyst of various atomic ratios prepared on carbon paper (geometric surface area of 0.53 cm^2). In this case, CV measurements up to 400 cycles were carried out. Before each test, the working solution ($0.1 \text{ mol}\cdot\text{L}^{-1}$ of ethanol and $0.5 \text{ mol}\cdot\text{L}^{-1}$ of H_2SO_4) [25] was carefully purged with high-purity nitrogen for 1 h and heated up to 80°C .

Results and Discussion

Pt-Sn/C Anode Characterization

XRD patterns of the synthesized catalyst powders are shown in Fig. 1. The diffraction peak at 20 – $25^\circ 2\theta$ observed in all the

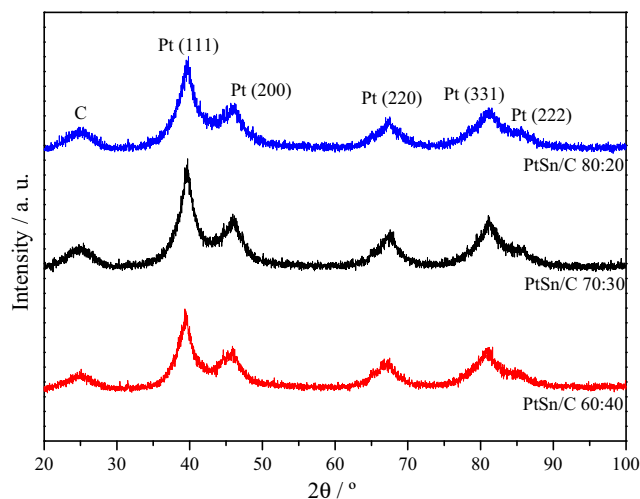


Fig. 1 XRD diffraction patterns of Pt-Sn/C catalysts with different Pt:Sn ratio as indicated in the figure

XRD patterns of the carbon-supported catalyst is attributed to the (002) plane of the hexagonal structure of carbon support [26]. It can be observed that only the reflections of face-centered cubic (fcc) platinum and hexagonal carbon support were present in the patterns of the Pt₆₀Sn₄₀/C, Pt₇₀Sn₃₀/C, and Pt₈₀Sn₂₀/C catalysts [1, 27–30]. Table 1 summarizes the main parameters obtained from XRD patterns. Lattice parameter was calculated from the (220) diffraction peak position, because this peak does not overlap with carbon reflections unlike the main (111) and (200) peaks. The lattice parameter was always larger than that for pure Pt/C commercial catalyst, 0.3913 nm [31]. However, these values are very close to the pure Pt/C (especially for the Pt-Sn 70:30 sample) suggesting that Sn is not integrated into the crystalline structure of the Pt and, therefore, that is present in amorphous state [1, 32]. Furthermore, the $2\theta_{\max}$ of the (220) peak was analyzed using a third-order polynomial, fit to the top of the peak. The peak maximum was found to be very close to $67.5^\circ 2\theta$ for pure Pt nanoparticles of the same size [19].

As reported earlier [19], for Pt_xSn_{1-x}/C prepared at a sodium hydroxide concentration of 0.2 M and initial pH of 11, only partial alloying between Pt and Sn was observed. There was no evidence of a separate crystalline phase of SnO₂ or Sn on XRD patterns, suggesting that tin is certainly present in an amorphous state, which has been demonstrated in previous studies [1, 19]. Considering the different atomic size, $R_{\text{Sn}} = 0.161$ nm and $R_{\text{Pt}} = 0.139$ nm, the inclusion of tin (bigger atomic size than platinum) would explain the slightly higher values in the lattice parameter [28]. The crystalline size of the catalyst was calculated using the (220) reflection peak according to Scherrer's formula. The crystalline size of Pt_xSn_{1-x}/C nanoparticles was found to be between 4.6 and 6 nm, demonstrating that the selected method was adequate for the preparation of nanoparticles. The Pt₇₀Sn₃₀/C anodic catalyst showed the lowest Pt particle size, which may contribute to an improved electrochemical reforming activity.

The electrochemical surface area (ECSA) is a key parameter for determining the catalytic activity of the manufactured electrocatalysts. ECSA of Pt_xSn_{1-x}/C catalysts was evaluated from cyclic voltammetry in 0.5 M H₂SO₄ solution at 50 mV·s⁻¹ (an example for Pt₇₀Sn₃₀/C is shown in the Supporting Information, Fig. S2) by measuring the charge in the hydrogen adsorption/desorption region after double-layer correction.

Table 1 Summary of characteristic properties of Pt-Sn catalysts

Catalyst	Nominal at. ratio (%)	Crystallite size (nm)	$2\theta_{\max}$ of (220) ($^\circ$)	Lattice parameter (nm)	Sn at. fraction in alloy
Pt ₆₀ Sn ₄₀	60:40	5.96	67.10	0.3927	0.11
Pt ₇₀ Sn ₃₀	70:30	4.64	67.45	0.3918	0.04
Pt ₈₀ Sn ₂₀	80:20	5.77	67.40	0.3933	0.16

After finding the charge, the ECSA was calculated using Eq. 1. Addition of Sn led to an increase of the platinum active surface area from 45.90 m²·g⁻¹ on the commercial 20% Pt/C catalyst to 57.99 m²·g⁻¹ for the case of the 70:30 Pt_xSn_{1-x}/C catalyst. It was larger than that exhibited by 60:40 and 80:20 Pt-Sn samples, 12.69 and 42.12 m²·g⁻¹, respectively. It is due to the smaller particles obtained for the former sample which led to well-dispersed Pt particles (as shown in the TEM image of the Supporting Information Fig. S3).

Electrochemical Reforming Experiments

In order to test the viability of these catalysts in the electrochemical reforming of alcohols, linear voltammetry experiments were performed at a constant temperature of 80 °C, ethanol concentration of 4 mol·L⁻¹, and a scan rate of 5 mV·s⁻¹ on three different MEAs prepared using the different Pt_xSn_{1-x}/C anodic catalyst. Figure 2a shows the variation of current density with the applied potential (0–1.3 V range), and Fig. 2b depicts the hydrogen production rate (experimental and

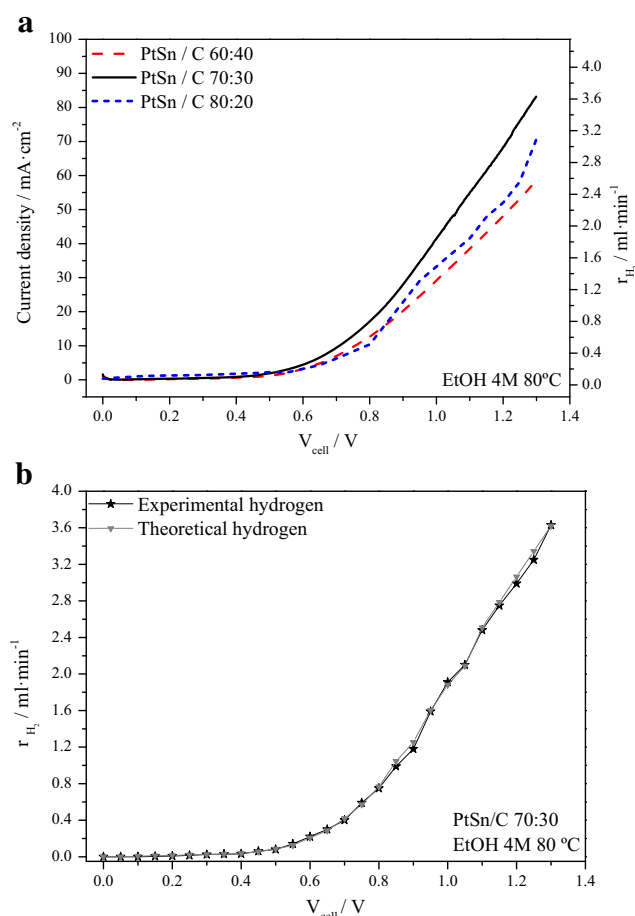


Fig. 2 Effect of the applied potential on **a** current density of three Pt-Sn/C catalysts and **b** hydrogen production (theoretical and experimental) for Pt₇₀Sn₃₀/C catalyst for 4 mol·L⁻¹ ethanol solution at 80 °C

theoretical) vs. the applied potential obtained for the Pt₇₀Sn₃₀/C catalyst. As it can be observed, ethanol electrooxidation began around 0.5 V with a continuous linear increase in the current density with the applied potential. This can be attributed to the electrochemical reforming of the ethanol, since no current density was obtained at any case by feeding pure water to the system (not shown here), which is in agreement with previous studies [8, 12]. As shown previously, this same trend was observed for all polarization curves for electrochemical reforming of alcohols in the PEM configuration [1, 8, 12]. It should be noted that using Faraday's law, the current density was related to the hydrogen produced at the cathode of the PEM cell. [8] These theoretical hydrogen production rate values were experimentally confirmed by separate experiments of gas-volumetric hydrogen flows (Fig. 2b). The reactions that take place in the electrochemical reforming of ethanol are detailed as follows (Eqs. 2 to 4) [1, 33]:



In addition, a hydrogen purity of 99.999% was confirmed by separate gas chromatography analyses. As expected, an increase in the applied potential led to higher current densities in all the cases and, consequently, higher hydrogen production rates. The best electrocatalytic behavior was observed in the MEA prepared with the Pt₇₀Sn₃₀/C anodic catalyst, which can be attributed to its lower particle size, higher ECSA values, and optimal surface composition and combination of Pt-Sn sites for the bifunctional mechanism of ethanol electrooxidation reaction on this kind of systems [17].

Figure 3 shows the influence of the temperature on the polarization curves for 4 mol·L⁻¹ ethanol for the MEA

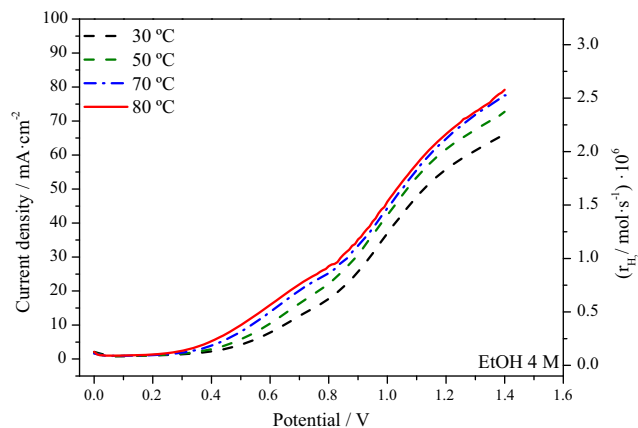


Fig. 3 Effect of the reaction temperature on the polarization of Pt-Sn/C catalyst for a 4 mol·L⁻¹ ethanol solution

prepared with Pt₇₀Sn₃₀/C catalyst. An increase in the reaction temperature resulted in an increase of the current density, as expected, thus improving the rate of production of hydrogen at the cathode of the cell. This improvement can be attributed to both the enhancement of the ethanol electrooxidation kinetics and the increase of the ionic conductivity of the membrane at fixed potential [8, 34]. Furthermore, the observed current densities were very similar to those previously reported for ethanol [1, 8], bio-ethanol [12], methanol [35], and ethylene glycol [14]. According to this test, a reaction temperature of 80 °C was selected for an ethanol concentration of 4 mol·L⁻¹ as the optimal reaction conditions for the following experiments. Temperatures above 80 °C were not explored in order to keep the humidity and the stability of the membrane, as will be shown below.

Long-Term Stability Test of Pt_xSn_{1-x}/C

Finally, in order to demonstrate the stability of the different MEAs, long-term electrochemical reforming experiments were carried out. The tests were run by a galvanostatic experiment ($I = 0.1$ A) in six consecutive cycles (of 8 h of duration of each one) with open circuit potential conditions (of 5 min of duration) between them, as explained in the “Experimental Section.” The cell was galvanostatically polarized at 80 °C with a current density of 16 mA cm⁻² (0.1 A) in different cycles. For each one, Fig. 4 shows the cell voltage evolution vs. time for the Pt_xSn_{1-x}/C sample. It can be observed that overall similar trends were observed for the different MEAs, i.e., in each cycle, an initial increase in the cell voltage was detected during the first minutes of the operation. It could be attributed to the catalyst

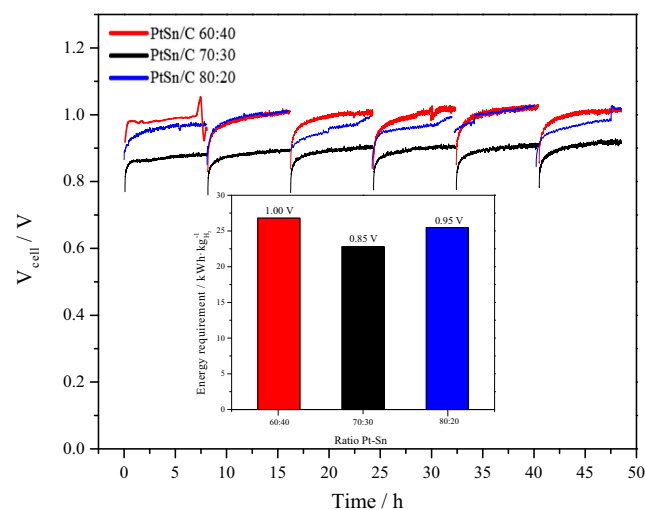


Fig. 4 Cyclic stability test and average energy requirement for three Pt-Sn/C anodic catalysts at 80 °C, 4 mol·L⁻¹ and current density of 16 mA·cm⁻²

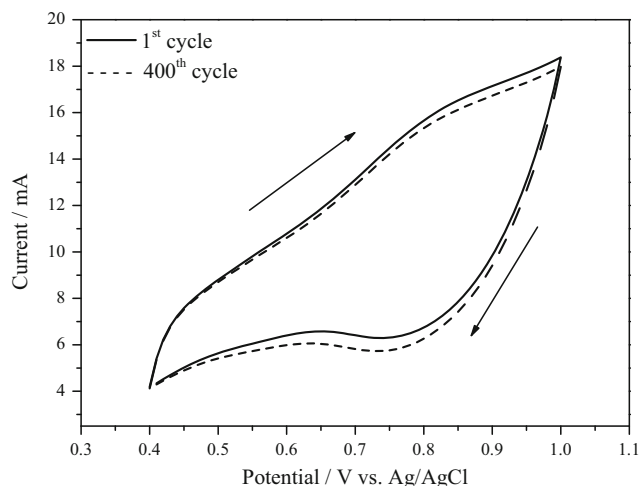


Fig. 5 Accelerated stress test for $0.1 \text{ mol}\cdot\text{L}^{-1}$ ethanol and $0.5 \text{ mol}\cdot\text{L}^{-1}$ H_2SO_4 at 80°C at the scan rate $20 \text{ mV}\cdot\text{s}^{-1}$

deactivation due to the accumulation of poisoning species adsorbed on the anodic catalyst surface [36, 37]. The deactivation phenomenon of this kind of systems is related to

the adsorption of reaction intermediates and products on the anodic catalyst, which resulted in an increase in the polarization resistance of the anode [38, 39]. After this first increase, the cell voltage was stable for the rest of the galvanostatic experiment, showing a reproducible behavior along the different cycles. In addition, in agreement with the previous results, the best electrocatalytic activity was obtained with the MEA prepared with the $70:30 \text{ Pt}_x\text{Sn}_{1-x}/\text{C}$, anodic catalyst, which required the lowest electrical potential for the same hydrogen production rate (same electrical current). As already mentioned, it could be attributed to its better textural and electrochemical properties, which favor the interaction between the catalyst surface and the ethanol molecules. Energy requirement estimations calculated from the average potential obtained during the galvanostatic experiments are shown on the inset of Fig. 4 for the three MEAs. The lowest energy consumption corresponded to MEA prepared with the $\text{Pt}_{70}\text{Sn}_{30}/\text{C}$ anodic catalyst, which achieved an energy requirement of $22.78 \text{ kW h kg}_{\text{H}_2}^{-1}$ at the explored conditions. In comparison, the energy requirement of a commercial PEM water

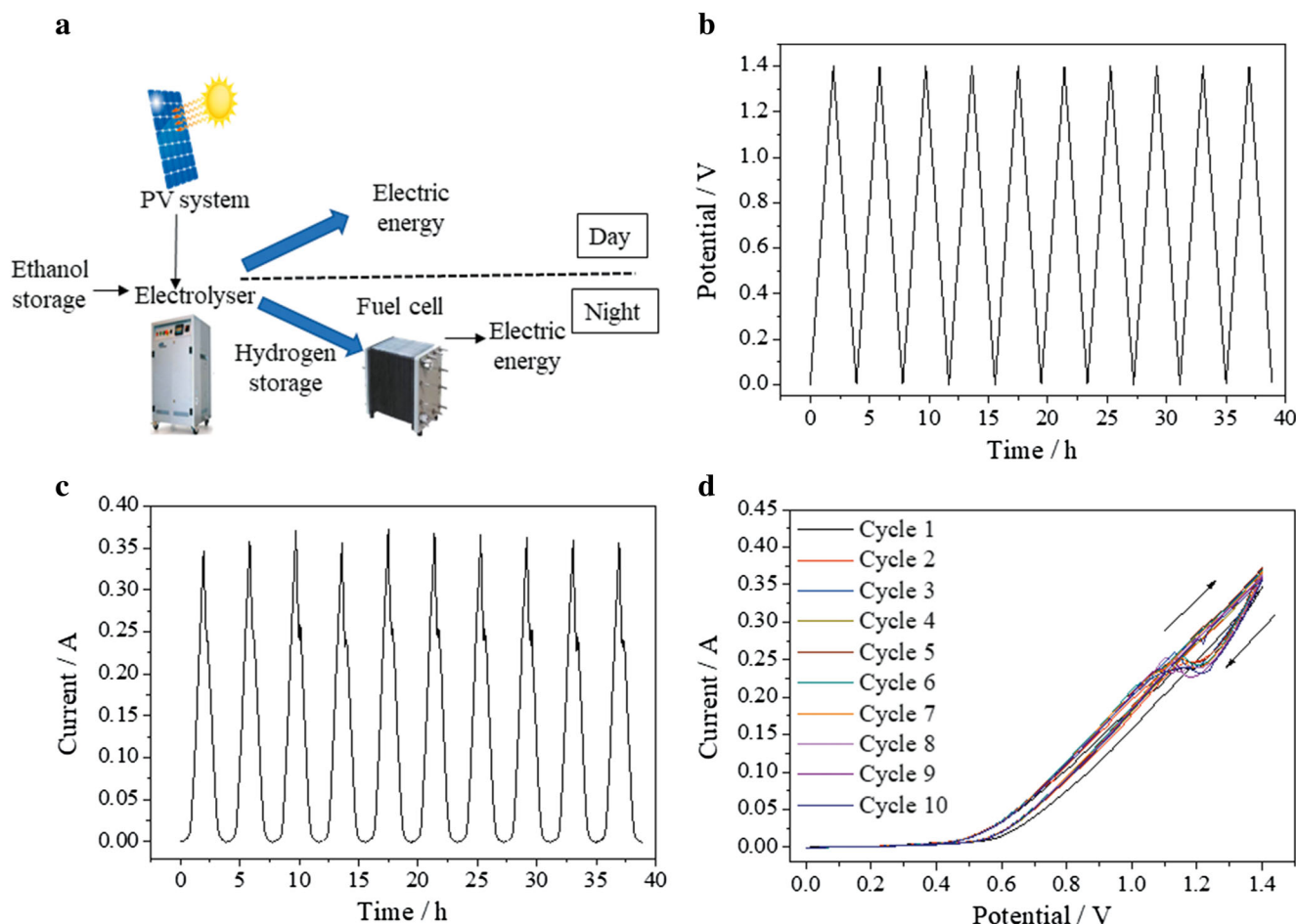


Fig. 6 Cyclic voltammetry measurements for typical solar profile simulations: **a** typical scheme to produce and store hydrogen using a renewable technology; **b** potential vs. time; **c** current vs. time; and **d** cyclic voltammetry for $4 \text{ mol}\cdot\text{L}^{-1}$ ethanol at 80°C at scan rate $0.19 \text{ mV}\cdot\text{s}^{-1}$

electrolyser stack is around 50–60 kWh·kg_{H₂}⁻¹ [40], which is much higher than that obtained in the present work for all the Pt_xSn_{1-x}/C synthesized anodic catalysts. The energy requirements showed in this study are similar to those shown in previous works for the electrochemical reforming of ethanol and bio-ethanol in acidic media [8, 12].

The stability of Pt₇₀Sn₃₀/C anodic catalyst was a subject of an accelerated stress test in a three-electrode glass cell [41], which tends to simulate and simplify the severe degradation that may occur during the operation of PEM electrolyzers. The experiment was carried out in the potential range of 0.4 to 1.0 V vs. Ag/AgCl at scan rate of 20 mV·s⁻¹ for 400 cycles. Figure 5 shows that for Pt₇₀Sn₃₀/C anodic catalyst, the current decreases by 3.21% from the first cycle to the last one, confirming good stability under the studied conditions.

Integration of Renewable Energy and Hydrogen Technology

Some additional experiments were performed using the MEA prepared from the Pt₇₀Sn₃₀/C anodic catalyst, looking for the integration of this technology with renewable energy sources (e.g., typical photovoltaic profiles). A possible scheme of this coupling technology is proposed in Fig. 6a. During the day, the photovoltaic cell and the electrolyser provide electric energy and hydrogen, respectively. The former can be directly used, and the excess of production can be used to electrolyze ethanol for the hydrogen production, which can be stored in order to be used at night in a fuel cell, thus providing electric energy when the solar energy it is not available. In order to simulate this procedure, cyclic voltammetry measurements were carried out simulating a typical solar profile at a very low scan rate of 0.19 mV·s⁻¹. The corresponding applied power (current × potential, not shown here) vs. time curve is very similar to that obtained by a daily solar photovoltaic cell, and hence, this behavior is close to a typical solar profile. In agreement with previous results, the obtained current and hydrogen rate showed to be proportional to the applied potential and power. The direct and fast response of the electrolyser allows the production of a higher amount of hydrogen as a higher amount of solar energy is produced. According to the voltammetry results, it can be observed that in the backward direction (Figs. 6c, d), a current peak is observed. This can be associated with the removal of carbonaceous species formed through incomplete oxidation in the forward scan [25, 42]. In addition, the hysteresis phenomena may also be attributed to slight differences on the anodic surface composition due to the reaction and adsorption of ethanol and/or intermediates during the anodic and cathodic scans after achieving the upper potential limit. However, the most interesting feature of the experiment is that a similar trend was obtained between the different cycles showing a good stability and a reproducible response of the system.

Therefore, it can be concluded that this technology could be suitably integrated with a renewable photovoltaic energy source in order to produce clean hydrogen and supply energy when the renewable energy is not available (e.g., during the night if solar energy is to be used).

Conclusions

This study can conclude the following aspects:

- Polyol reduction method was used for the synthesis of different Pt_xSn_{1-x}/C anodic catalysts in order to produce hydrogen from electrochemical reforming of ethanol in a PEM cell configuration.
- Pt_xSn_{1-x}/C anodic catalysts present a (fcc) Pt and amorphous Sn structure, with a relatively small particle size from 4.6 to 6 nm.
- Pt_xSn_{1-x}/C anodic catalyst with a 70:30 nominal atomic ratio showed the highest electrochemical reforming activity. This could be attributed to the smallest particle size, as well as the highest electrochemical active surface area (ECSA).
- Durability and the stability of the MEAs prepared with the synthesized Pt_xSn_{1-x}/C anodic catalysts were evaluated for 48 h of operation in six consecutive cycles of 8 h in duration. Moreover, the proposed system presents a lower energy requirement than commercial water electrolysis systems, so it can be considered a promising technology to produce high-purity hydrogen from the electrochemical reforming of ethanol.
- Possible coupling of this technology with renewable solar energy sources (e.g., photovoltaic) has been demonstrated in order to produce clean hydrogen and supply energy when the renewable energy is not available (e.g., during the night if solar energy is to be used).

Funding Information We acknowledge the Spanish Ministry of Economy and Competitiveness (project CTQ2016-75491-R) for the financial support. A. B. Calcerrada would like also to thank the Junta de Comunidades de Castilla-La Mancha (JCCM) and the European Social Fund for the financial support.

References

1. A.R. de la Osa, A.B. Calcerrada, J.L. Valverde, E.A. Baranova, A. de Lucas-Consuegra, Electrochemical reforming of alcohols on nanostructured platinum-tin catalyst-electrodes. *Appl. Catal. B Environ.* **179**, 276–284 (2015)
2. C. Lamy, B. Guenot, M. Cretin, and G. Pourcelly. *A kinetics analysis of methanol oxidation under electrolysis/fuel cell working conditions*. In *Symposium on Electrocatalysis 7 - 227th ECS Meeting*. 2015. Electrochem. Soc. Inc.

3. C.R. Cloutier, D.P. Wilkinson, Electrolytic production of hydrogen from aqueous acidic methanol solutions. *Int. J. Hydrog. Energy* **35**(9), 3967–3984 (2010)
4. A.T. Pham, T. Baba, T. Shudo, Efficient hydrogen production from aqueous methanol in a PEM electrolyzer with porous metal flow field: influence of change in grain diameter and material of porous metal flow field. *Int. J. Hydrogen Energy* **38**(24), 9945–9953 (2013)
5. A.T. Marshall, R.G. Haverkamp, Production of hydrogen by the electrochemical reforming of glycerol–water solutions in a PEM electrolysis cell. *Int. J. Hydrog. Energy* **33**(17), 4649–4654 (2008)
6. S. Kongjao, S. Damronglerd, M. Hunsom, Electrochemical reforming of an acidic aqueous glycerol solution on Pt electrodes. *J. Appl. Electrochem.* **41**(2), 215–222 (2011)
7. J. de Paula, D. Nascimento, J.J. Linares, Influence of the anolyte feed conditions on the performance of an alkaline glycerol electroreforming reactor. *J. Appl. Electrochem.* **45**(7), 689–700 (2015)
8. A. Caravaca, F.M. Sapountzi, A. De Lucas-Consuegra, C. Molina-Mora, F. Dorado, J.L. Valverde, Electrochemical reforming of ethanol–water solutions for pure H₂ production in a PEM electrolysis cell. *Int. J. Hydrog. Energy* **37**(12), 9504–9513 (2012)
9. C. Lamy, T. Jaubert, S. Baranton, and C. Coutanceau, Clean hydrogen generation through the electrocatalytic oxidation of ethanol in a proton exchange membrane electrolysis cell (PEMEC): effect of the nature and structure of the catalytic anode. *J. Power Sources*, 2014. 245(0): p. 927–936
10. A. De Lucas-Consuegra, A.R. De La Osa, A.B. Calcerrada, J.J. Linares, D. Horwat, A novel sputtered Pd mesh architecture as an advanced electrocatalyst for highly efficient hydrogen production. *J. Power Sources* **321**, 248–256 (2016)
11. A. Jablonski, A. Lewera, Electrocatalytic oxidation of ethanol on Pt, Pt–Ru and Pt–Sn nanoparticles in polymer electrolyte membrane fuel cell–role of oxygen permeation. *Appl. Catal. B Environ.* **115–116**, 25–30 (2012)
12. A. Caravaca, A. De Lucas-Consuegra, A.B. Calcerrada, J. Lobato, J.L. Valverde, F. Dorado, From biomass to pure hydrogen: electrochemical reforming of bio-ethanol in a PEM electrolyser. *Appl. Catal. B Environ.* **134–135**, 302–309 (2013)
13. Y.X. Chen, A. Lavacchi, H.A. Miller, M. Bevilacqua, J. Filippi, M. Innocenti, A. Marchionni, W. Oberhauser, L. Wang, F. Vizza, Nanotechnology makes biomass electrolysis more energy efficient than water electrolysis. *Nat. Commun.* **5** (2014)
14. A. De Lucas-Consuegra, A.B. Calcerrada, A.R. De La Osa, J.L. Valverde, Electrochemical reforming of ethylene glycol. Influence of the operation parameters, simulation and its optimization. *Fuel Process. Technol.* **127**, 13–19 (2014)
15. L. Jiang, A. Hsu, D. Chu, R. Chen, Ethanol electro-oxidation on Pt/C and PtSn/C catalysts in alkaline and acid solutions. *Int. J. Hydrogen Energy* **35**(1), 365–372 (2010)
16. A.O. Neto, R.R. Dias, M.M. Tusi, M. Linardi, E.V. Spinacé, Electro-oxidation of methanol and ethanol using PtRu/C, PtSn/C and PtSnRu/C electrocatalysts prepared by an alcohol-reduction process. *J. Power Sources* **166**(1), 87–91 (2007)
17. F. Vigier, C. Coutanceau, F. Hahn, E.M. Belgsir, C. Lamy, On the mechanism of ethanol electro-oxidation on Pt and PtSn catalysts: electrochemical and in situ IR reflectance spectroscopy studies. *J. Electroanal. Chem.* **563**(1), 81–89 (2004)
18. C. Lamy, S. Rousseau, E.M. Belgsir, C. Coutanceau, J.M. Léger, Recent progress in the direct ethanol fuel cell: development of new platinum–tin electrocatalysts. *Electrochim. Acta* **49**(22–23 SPEC. ISS.), 3901–3908 (2004)
19. E.A. Baranova, T. Amir, P.H.J. Mercier, B. Patarachao, D. Wang, Y. Le Page, Single-step polyol synthesis of alloy Pt₇Sn₃ versus bi-phase Pt/SnOx nano-catalysts of controlled size for ethanol electro-oxidation. *J. Appl. Electrochem.* **40**(10), 1767–1777 (2010)
20. E. Antolini, E.R. Gonzalez, The electro-oxidation of carbon monoxide, hydrogen/carbon monoxide and methanol in acid medium on Pt–Sn catalysts for low-temperature fuel cells: a comparative review of the effect of Pt–Sn structural characteristics. *Electrochim. Acta* **56**(1), 1–14 (2010)
21. E.A. Baranova, C. Bock, D. Ilin, D. Wang, B. MacDougall, Infrared spectroscopy on size-controlled synthesized Pt-based nano-catalysts. *Surf. Sci.* **600**(17), 3502–3511 (2006)
22. C. Bock, C. Paquet, M. Couillard, G.A. Botton, B.R. MacDougall, Size-selected synthesis of PtRu nano-catalysts: reaction and size control mechanism. *J. Am. Chem. Soc.* **126**(25), 8028–8037 (2004)
23. P. Rupa Kasturi, R. Kalai Selvan, Y.S. Lee, Pt decorated: *Artocarpus heterophyllus* seed derived carbon as an anode catalyst for DMFC application. *RSC Adv.* **6**(67), 62680–62694 (2016)
24. J. Lobato, H. Zamora, J. Plaza, P. Cañizares, M.A. Rodrigo, Enhancement of high temperature PEMFC stability using catalysts based on Pt supported on SiC based materials. *Appl. Catal. B Environ.* **198**, 516–524 (2016)
25. R.M. Abdel Hameed, A.E. Fetohi, R.S. Amin, K.M. El-Khatib, Promotion effect of manganese oxide on the electrocatalytic activity of Pt/C for methanol oxidation in acid medium. *Appl. Surf. Sci.* **359**, 651–663 (2015)
26. L. Jiang, A. Hsu, D. Chu, R. Chen, Oxygen reduction reaction on carbon supported Pt and Pd in alkaline solutions. *J. Electrochem. Soc.* **156**(3), B370–B376 (2009)
27. M. Carmo, A.R. dos Santos, J.G.R. Poco, M. Linardi, Physical and electrochemical evaluation of commercial carbon black as electrocatalysts supports for DMFC applications. *J. Power Sources* **173**(2), 860–866 (2007)
28. W. Zhou, Z. Zhou, S. Song, W. Li, G. Sun, P. Tsiakaras, Q. Xin, Pt based anode catalysts for direct ethanol fuel cells. *Appl. Catal. B Environ.* **46**(2), 273–285 (2003)
29. M. Chatterjee, A. Chatterjee, S. Ghosh, I. Basumallick, Electro-oxidation of ethanol and ethylene glycol on carbon-supported nano-Pt and -PtRu catalyst in acid solution. *Electrochim. Acta* **54**(28), 7299–7304 (2009)
30. E.A. Baranova, Y. Le Page, D. Ilin, C. Bock, B. MacDougall, P.H.J. Mercier, Size and composition for 1–5 nm Ø PtRu alloy nanoparticles from Cu K α X-ray patterns. *J. Alloys Compd.* **471**(1–2), 387–394 (2009)
31. H. Li, G. Sun, L. Cao, L. Jiang, Q. Xin, Comparison of different promotion effect of PtRu/C and PtSn/C electrocatalysts for ethanol electro-oxidation. *Electrochim. Acta* **52**(24), 6622–6629 (2007)
32. J. Lobato, P. Cañizares, M.A. Rodrigo, J.J. Linares, Study of different bimetallic anodic catalysts supported on carbon for a high temperature polybenzimidazole-based direct ethanol fuel cell. *Appl. Catal. B Environ.* **91**(1–2), 269–274 (2009)
33. F.M. Sapountzi, M.N. Tsampas, H.O.A. Fredriksson, J.M. Gracia, J.W. Niemantsverdriet, Hydrogen from electrochemical reforming of C1–C3 alcohols using proton conducting membranes. *Int. J. Hydrog. Energy* **42**(16), 10762–10774 (2017)
34. S. Song, W. Zhou, J. Tian, R. Cai, G. Sun, Q. Xin, S. Kontou, P. Tsiakaras, Ethanol crossover phenomena and its influence on the performance of DEFC. *J. Power Sources* **145**(2), 266–271 (2005)
35. G. Sasikumar, A. Muthumeenal, S.S. Pethaiah, N. Nachiappan, R. Balaji, Aqueous methanol electrolysis using proton conducting membrane for hydrogen production. *Int. J. Hydrog. Energy* **33**(21), 5905–5910 (2008)
36. J. Datta, A. Dutta, S. Mukherjee, The beneficial role of the cometal Pd and Au in the carbon-supported PtPdAu catalyst toward promoting ethanol oxidation kinetics in alkaline fuel cells: Temperature effect and reaction mechanism. *J. Phys. Chem. C* **115**(31), 15324–15334 (2011)

37. A. Dutta, S.S. Mahapatra, J. Datta, High performance PtPdAu nano-catalyst for ethanol oxidation in alkaline media for fuel cell applications. *Int. J. Hydrog. Energy* **36**(22), 14898–14906 (2011)
38. S. Song, G. Wang, W. Zhou, X. Zhao, G. Sun, Q. Xin, S. Kontou, P. Tsiakaras, The effect of the MEA preparation procedure on both ethanol crossover and DEFC performance. *J. Power Sources* **140**(1), 103–110 (2005)
39. J. Lobato, P. Cañizares, M.A. Rodrigo, J.J. Linares, Testing a vapour-fed PBI-based direct ethanol fuel cell. *Fuel Cells* **9**(5), 597–604 (2009)
40. M. Carmo, D.L. Fritz, J. Mergel, D. Stolten, A comprehensive review on PEM water electrolysis. *Int. J. Hydrog. Energy* **38**(12), 4901–4934 (2013)
41. S. Zhang, X.Z. Yuan, J.N.C. Hin, H. Wang, K.A. Friedrich, M. Schulze, A review of platinum-based catalyst layer degradation in proton exchange membrane fuel cells. *J. Power Sources* **194**(2), 588–600 (2009)
42. L. Zhang, D. Xia, Electrocatalytic activity of ordered intermetallic PtSb for methanol electro-oxidation. *Appl. Surf. Sci.* **252**(6), 2191–2195 (2006)